Nanoscale

PAPER

View Article Online
View Journal | View Issue

Cite this: *Nanoscale*, 2017, **9**, 8489

In situ IR-spectroscopy as a tool for monitoring the radical hydrosilylation process on silicon nanocrystal surfaces†

Julian Kehrle,‡[a] Simon Kaiser,‡[a] Tapas K. Purkait,[b] Malte Winnacker,[a] Tobias Helbich,[a] Sergei Vagin,[a] Jonathan G. C. Veinot*[c] and Bernhard Rieger*[a]

Received 30th March 2017,
Accepted 19th May 2017

DOI: 10.1039/c7nr02265d

rsc.li/nanoscale

Among a variety of SiNC functionalization methods, radical initiated grafting is very promising due to its straightforward nature and low propensity to form surface oligomers. In the present study, we employed *in situ* IR spectroscopy in combination with visible light transmittance measurements to investigate the radical induced grafting process on the well-defined SiNCs. Our findings support the proposed model: unfunctionalized hydride-terminated SiNCs form agglomerates in organic solvents, which break up during the grafting process. However, clearing of the dispersion is not a valid indicator for complete surface functionalization. Furthermore, radical-initiated grafting reactions in which azobisisobutyronitrile (AIBN) is the initiator are strongly influenced by external factors including initiator concentration, grafting temperature, as well as substrate steric demand. The monomer concentration was proven to have a low impact on the grafting process. Based on these new insights an underlying mechanism could be discussed, offering an unprecedented view on the functionalization of SiNC surfaces *via* radical initiated hydrosilylation.

Introduction

Silicon nanocrystals (SiNCs) have emerged as a class of non-toxic, electrochemically stable quantum dots.[1,2] It is well-established that the optical and electronic properties of these promising materials may be tuned by varying the particle size and surface chemistry.[3–6] As a result of their exquisitely tunable optoelectronic response, a variety of prototype applications have been demonstrated including sensors,[7,8] bioimaging,[9–11] and light-emitting diodes (LEDs).[12–14]

The most widely investigated methods for functionalizing SiNCs are based upon variations (*e.g.*, metal catalyzed,[15] thermally-[16–19] and photochemically-induced,[20,21] radical initiated,[22,23] *etc.*) of the general hydrosilylation reaction that involves hydrogen-terminated SiNCs (H-SiNCs); each procedural variant has its own advantages and challenges.[6,24] For example, residual metal catalyst impurities can compromise SiNC optical response.[25] Thermal and photoinitiated hydrosilylations apparently evade this issue. Thermal grafting of olefins and alkynes is most often performed on a neat substrate and, while it leads to surface modification, surface oligomerization and solution phase homopolymerization have been identified as potential limitations.[16,19] Oligomerization is minimized (if not eliminated) by applying photoinduced protocols, however, limited surface coverage often results and the NC surfaces remain susceptible to deleterious reactivity (*e.g.*, oxidation) that can lead to altered and unpredictable properties.[20,26] Furthermore, the general photochemical procedure is not effective for SiNCs of all sizes and substrates.[21] Of late there has been increased interest in metal-free catalysts or radical initiators that offer efficient surface coverage and short reaction times, however, even those can lead to unexpected consequences related to optical response.[20,27]

Despite the impressive advances, questions remain regarding the efficacy of SiNC surface modification; perhaps the chief among them is: how do SiNC surface reactions generally proceed? Typically, the reaction progress is evaluated qualitatively by monitoring the optical transparency of the reaction mixture.[22,23] The basis for this analysis is the assumption that the formation of sterically stabilized SiNC colloids will induce a "clearing" of the formerly turbid dispersion of H-SiNCs. SiNC grafting mechanisms have mostly been derived from flat silicon surfaces[22,23,28–31] or focused on thermal[32] and photoinitiated reactions.[20,21] To date, no quantitative evaluation of the reaction progress has been presented to support these findings for radical initiated SiNC surface grafting. To address

[a]*Catalysis Research Center/WACKER-Lehrstuhl für Makromolekulare Chemie, Technische Universität München, Lichtenbergstraße 4, 85747 Garching bei München, Germany. E-mail: rieger@tum.de*
[b]*Department of Chemistry, Johns Hopkins University, Baltimore, MD 21218, USA*
[c]*Department of Chemistry, University of Alberta, Edmonton, Alberta T6G 2G2, Canada. E-mail: jveinot@ualberta.ca*

†Electronic supplementary information (ESI) available: Further synthetic procedure and analysis (*e.g.* UV-VIS, PL, TEM, HR-TEM, DLS, ATR-IR, XPS, NALDI, TGA and elemental analysis). See DOI: 10.1039/c7nr02265d

‡J. K. and S. K. contributed equally.

this concern, we describe a detailed IR study of hydrosilylation reactions of a wide range of vinylsilanes on the surfaces of well-defined H-SiNCs ($d \sim 3$ nm) initiated using azobisisobutyronitrile (AIBN).

Experimental

Material characterization and instrumentation

Materials. All chemicals were purchased from Sigma Aldrich and ABCR and used without purification if not stated otherwise. Solvents were dried using a solvent purification system LABmaster 130 from MBraun. Triphenylvinylsilane,[33,34] 1,1,1,3,3-pentamethyl-3-vinyldisiloxane[35] and 1,1,1,5,5,5-hexamethyl-3-(trimethylsiloxy)-3-vinyltrisiloxane[36] were synthesized according to the known literature procedures (ESI section 1†). Vinylsilanes were dried over molecular sieves and distilled or recrystallized. AIBN was recrystallized from methanol prior to use. Functionalization reactions were performed under an inert gas using dry solvents. Centrifugations were performed using ETFE centrifuge tubes purchased from Roth, to prevent solvatization of oligoolefins from conventional centrifugation tubes. Schlenk tubes for *in situ* ATR-IR measurements were produced from the glassblower of the TUM, department of chemistry.

Attenuated total reflectance infrared (ATR-IR) spectra were measured by drop coating of the sample on the probe using a nitrogen cooled VERTEX 70 FTIR spectrometer from Bruker and a Platinum ATR unit (s – strong, m – medium and w – weak). *In situ* IR spectroscopy was performed on a liquid nitrogen cooled Mettler Toledo ReactIR 45 m with a silicon ATR probe into a SiNC-toluene dispersion. Measurements were performed every 30 seconds applying 125 scans.

UV/Vis spectra were recorded on a Cary 50 from Varian. Transmittance measurements were performed in the absorbance mode using a wavelength of 800 nm.

Gel permeation chromatography (GPC) was obtained from a Varian PL-GPS 50 Plus equipped with two PLgel MIXED-C columns using tetrahydrofuran with a flow rate of 1 mL min^{-1}. Calibration was performed using polystyrene standards.

Functionalization of SiNCs

600 mg of the SiNC composite are liberated by the HF etching procedure, redispersed in 6 mL of toluene and transferred into three *in situ* IR Schlenk tubes (ESI Table S2†). Afterwards, vinylsilane and toluene are added to provide a substrate concentration of 1.26 mmol mL^{-1} and a SiNC concentration of 1 ± 0.1 mg mL^{-1} at a fixed volume of 3.6 mL. The reaction mixture is then degassed using three freeze–pump–thaw cycles and ultrasonicated for 1 h. Subsequently the *in situ* IR probe is dipped into the dispersion under an Ar flow. The system is heated to the desired temperature (mainly 70 °C) and stirred at 400 min^{-1} to equilibrate. After 10 min, a solution of AIBN of the desired concentration (mainly 24.4 μmol dissolved in 0.20 mL dry, degassed toluene) is added *via* a syringe. The addition of AIBN defines t = 0 min. The characteristic Si–H band between 2158 and 2040 cm^{-1} is monitored. A two-point baseline has been used to integrate the signal.

Results and discussion

Reactivity of Si–H nanocrystal agglomerates

To quantitatively evaluate the progression of radical initiated hydrosilylation reactions on SiNCs it is preferable to monitor the cases involving a molecular reagent that readily attaches to the NC surfaces and exhibits a low propensity for solution-phase polymerization; it is also important to employ a radical initiator with well-understood reactivity. Vinylsilanes are an ideal substrate for the present study, because it is established that the pendant vinyl group affords effective functionalization of SiNCs[37] with low solution polymerization.[38] Similarly, the decomposition dynamics of the radical initiator azobisisobutyronitrile (AIBN) are intensely studied.[39]

In our study we used SiNCs prepared *via* thermal disproportionation of hydrogen silsesquioxane followed by etching with alcoholic HF.[18] After extraction, the resulting H-SiNCs are isolated by centrifugation and dispersed in dry toluene; subsequently, known quantities of vinylsilane precursors (*e.g.*, trimethylvinylsilane, TMVS) or other alkenes (ESI Part 1.2.1, Table S2†), and AIBN were added to the turbid reaction mixture. Finally, the reaction progress was monitored by *in situ* ATR-IR spectroscopy (ESI Fig. S1†).

Fundamental changes are observed in the IR spectrum of SiNCs upon functionalization with various substrates (Fig. 1) and monitoring key features such as the Si–H absorption band using *in situ* IR spectroscopy offers a unique opportunity to track the reaction progress (ESI Fig. S1†). In this regard, time resolved *in situ* IR analysis was performed on a known volume of a dispersion of H-SiNCs ($d \sim 3$ nm; 1 mg mL^{-1})[18] with a total Si–H concentration of 18.8 μmol mL^{-1} (ESI section 2.2†)

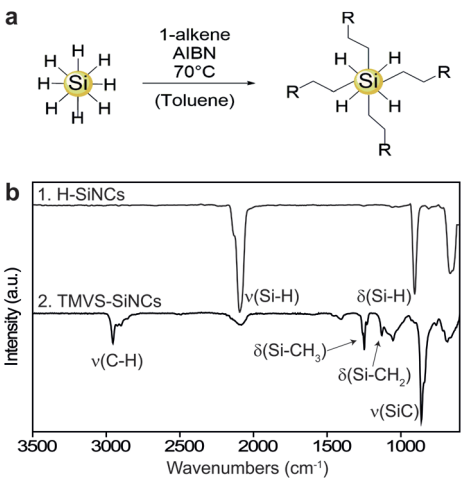

Fig. 1 (a) Schematic illustration of the radical SiNC functionalization process using trimethylvinylsilane as the substrate. (b) Attenuated total reflectance infrared (ATR-IR) spectrum of H-SiNCs (1) and TMVS-SiNCs (2).

and varying concentrations of vinylsilanes or alkenes, and AIBN (ESI Table S1†).

To correlate functionalization with optical clarity of the reaction mixture simultaneous time resolved visible light (800 nm) transmittance and *in situ* IR spectroscopy measurements were performed using 1-hexene (Fig. 2a, I), trimethylvinylsilane (TMVS, II), and triphenylvinylsilane (TPVS, III). With a decreasing size of SiNC agglomerates, particle dispersions appear transparent due to a weaker Rayleigh scattering; this observation has previously been used as a qualitative indicator for effective functionalization of SiNCs and was assumed to result from a nearly complete surface reaction.[22,23]

The performed kinetic studies clearly demonstrate the difference between the "clearing period" of the dispersion and the time required for complete functionalization. This effect depends on the steric bulk of the substrate, presumably because surface reactions involving bulkier olefins are slower. For instance, for the bulky TPVS (Fig. 2a, III) the dispersion becomes already clear after ~110 min, while the disappearance of the Si–H signal needs additional 231 min. For the sterically less bulky TMVS(II) the clarification time reduces to ~100 min, but complete Si–H consumption is reached after another 97 min. The influence of the steric bulk of the substrate becomes more obvious when using 1-hexene(I), which becomes transparent after ~55 min (plus 54 min for Si–H conversion). Fig. 2b shows the proposed underlying reaction sequence of the following procedure: the Si–H groups of the "outer surface" of the agglomerates react first. This induces a breaking up of these large particles and generates continuously "fresh" Si–H groups. Once the agglomerates reach a critical size, the dispersions become clear while the conversion of Si–H groups proceeds on the individual nanocrystals.

Radical formation and their reactions

To gain further insight into the general nature of radical initiated hydrosilylation grafting processes on H-SiNC surfaces, several parameters were varied and the reactions were again monitored using *in situ* IR spectroscopy. The influence of the present radical concentrations on the SiNC functionalization was determined by varying the AIBN concentrations (at constant temperatures) and reaction temperatures (at a constant AIBN concentration; ESI Table S2,† entries 1 and 2).[39] Fig. 3a shows that an increasing AIBN concentration affords higher functionalization rates. However, the rapidity of the functionalization converges and reaches a maximum at high AIBN concentrations (see Fig. 3a, I, II). Therefore, we propose that at very high AIBN concentrations, cleavage of SiNC agglomerates becomes the rate determining step.

As is the case with some literature proposals,[22,23] at lower AIBN concentrations surface hydrosilylation reactions proceed *via* a chain reaction mechanism, and radical efficiencies of the present SiNC surface reactions exceed unity as a consequence of reduced termination reactions (Fig. 3b, ESI Tables S9 and S10†).[40,41] The same proposal holds true, when the influence of the temperature on AIBN decomposition is considered (Fig. 3c). At 100 °C complete functionalization of H-SiNCs occurs within 10 minutes, although with a lower radical efficiency; at 50 °C the reactions require approximately 23 h.

In addition to SiNC surface reactions, the radical initiators formed by AIBN decomposition can also induce radical chain reactions in solution. Size exclusion chromatography (SEC) was used to investigate the possibility of solution phase substrate oligomerization (Fig. 3e and f). Samples evaluated included: (1) a reaction mixture prepared using AIBN and the substrate (*i.e.*, no SiNCs); (2) a reaction mixture using AIBN, the substrate and SiNCs; and (3) a purified functionalized SiNC fraction. TMVS forms small amounts of oligomers in solution, independent of the presence of SiNCs (Fig. 3e). The as-synthesized SiNCs in a mixture with solution oligomer (2) show lower molecular weights than the purified SiNCs (3), where small SiNCs were washed away during purification. Similar observations, but higher molecular weight fractions of polymers and oligomers were noted for triethoxyvinylsilane (TEVS; Fig. 3f).[38]

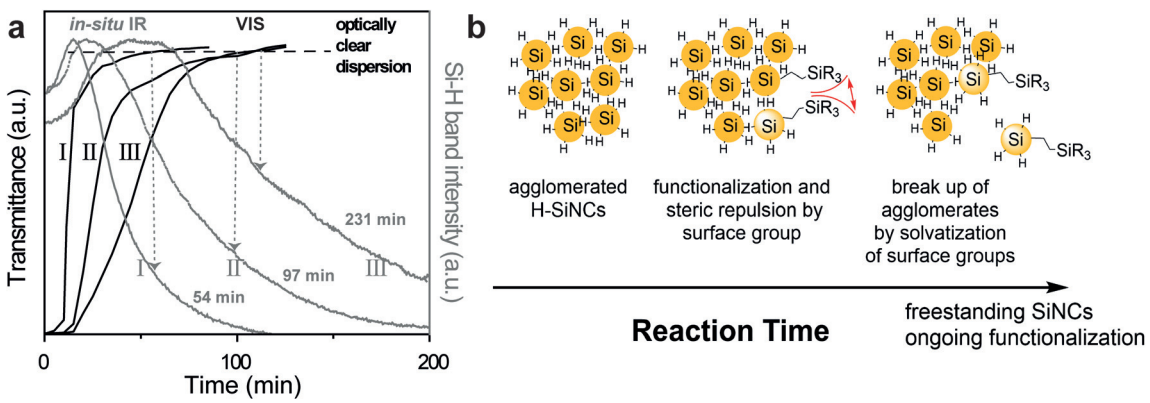

Fig. 2 (a) Comparison of the VIS-transmittance measurements using λ = 800 nm (black) and *in situ* IR evolutions of the Si–H band at 2100 cm^{-1} (grey) for 1-hexene (I), TMVS (II) and TPVS (III) measured during the functionalization reaction of hydride terminated SiNCs. (b) Schematic illustration of the agglomerate break-up process leading to clear reaction mixtures.

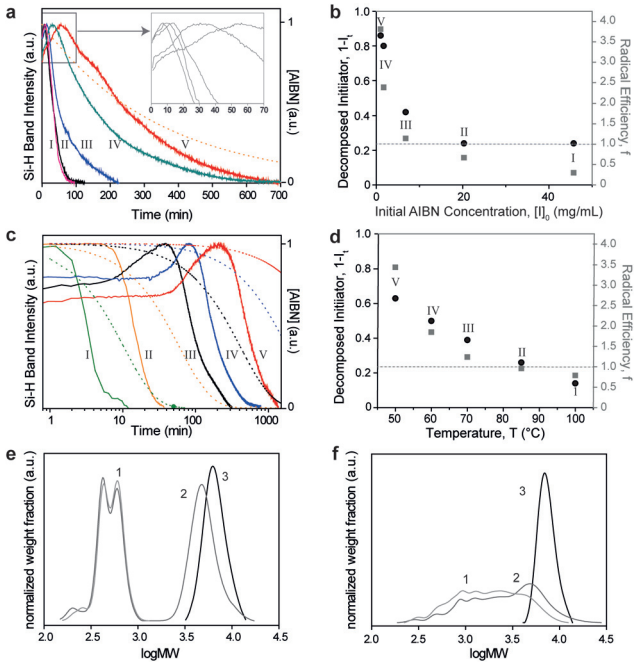

Fig. 3 (a) Evolution of the SiH band (2100 cm^{-1}) intensity during functionalization of hydride-terminated SiNCs with TMVS at 70 °C with AIBN concentrations of 45.7 μmol mL^{-1} (I), 20.3 μmol mL^{-1} (II), 6.8 μmol mL^{-1} (III), 1.7 μmol mL^{-1} (IV) and 1.0 μmol mL^{-1} (V) (inset: magnification of the starting evolutions). (b) Relative concentrations of the decomposed initiator 1-It at complete Si–H conversion and corresponding radical efficiencies f based upon 1-It (ESI Table S9†). (c) Evolution of the SiH band (2100 cm^{-1}) intensity during functionalization of hydride terminated SiNCs with a constant AIBN concentration of 6.8 μmol mL^{-1} at reaction temperatures of 100 °C (I), 85 °C (II), 70 °C (III), 60 °C (IV) and 50 °C (V); dashed lines show the respective AIBN decomposition rate calculated from the rate constants. (d) 1-It after complete Si–H conversion and corresponding f (ESI Table S10†). Size exclusion chromatogram (THF, relative to polystyrene standards) of the AIBN initiated reaction of (e) TMVS and (f) TEVS in toluene at 70 °C in the absence of SiNCs (1) and with SiNCs present (2 – workup in vacuum; 3 – workup *via* precipitation–centrifugation).

Sterics: the key to reaction rates

Stefanac *et al.* showed that under radical conditions vinyl oligomerization of diphenylvinylsilane is favored over its intermolecular hydrosilylation reaction.[38] Thus, in the SiNC surface reaction one would expect that after initiation, solution oligomerization of vinylsilanes dominates over surface grafting, consistent with the present SEC experiments.

Additionally, the surface hydrosilylation rates should correlate with the accessibility of the Si–H groups and the steric demand of the activating radical.[42] As a result of the surface hydrogen atom abstraction being a heterogeneous process (due to the necessity for the breakup of H-SiNC agglomerates), the steric demand of the activating radical was expected to play a crucial role for the reaction rates.[42] Hence, we propose that the available oligomer radicals would induce the formation of silyl radicals from H-SiNCs. To verify this proposal, a series of substrates with varying steric properties were investigated using *in situ* IR.

At first, the rates of 1-hexene and 1-dodecene, well-known substrates for SiNC surface functionalization, were compared to the TMVS reactivity (Fig. 4a).[22] All surface reactions run faster with 1-hexene (~110 min) and with slower rates for 1-dodecene (~160 min) and TMVS (~200 min). As a result of steric shielding of the surface from the solution formed oligomer radicals, the rates slow down. Steric surface shielding arises from conformational flexibilities of surface bonded dodecyl groups or dodecyl oligomer moieties.

Because of the observed influence of the nature of the olefin substrate and stability of bulky radicals on the surface functionalization rate, several vinylsilanes with different steric demands were investigated. The substrate bulkiness was increased upon changing the substitution around the central silicon of the substrate (ESI section 1.2; Table S2,† entry 3). Fig. 4b–d show conclusively that bulky substituents decrease the reaction rates compared to TMVS (~200 min). For example, dimethylphenylvinylsilane (DMPVS) needs 270 min and its bigger homologue triphenylvinylsilane (TPVS) needs 330 min. Upon ethoxy substitution, the gap between the single substituted dimethylethoxyvinylsilane (DMEVS) enhances from 220 min to 380 min for the triethoxyvinylsilane (TEVS). Most significant changes were observed, when trimethylsiloxy substituents were employed: pentamethylvinyldisiloxane (PMVDS) reacted in 280 min while the trisubstituted tris(trimethylsiloxy) vinylsilane (TTMSVS) needed ~31 h. This trend is further emphasized by decreasing surface coverages, decreasing the degrees of substitution (relative number of substituted Si–H groups by ligand molecules), as well as reduced radical efficiencies for bulkier substituents within the homologue series (as shown in Fig. 4e and f and ESI Tables S7 and S8†). In this regard, TTMSVS, which has a shielded vinyl group, exhibits the lowest reaction rate, degree of substitution (10%) and initiator efficiency (0.13) of all samples.

The behavior of bulky vinylic substrates toward the SiNC functionalization is similar to the findings for molecular silanes, where the silyl radical formation is highly dependent on the sterics of the incoming radical.[42] Furthermore, H-SiNCs only react with 2,2,6,6-tetramethylpiperidinyloxyl (TEMPO) if a radical initiator is available, but no reactivity was observed when olefins were added.[22] Hence, a capturing of solved radical species by TEMPO is dominant over surface reactions. This underlines the hypothesis that homolytic Si–H cleavage on SiNC surfaces occurs from oligomers or alkyl based radicals rather than from free butyronitrile radicals. Thus, we suggest that the Si–H cleavage by oligomer radicals is the rate-determining step in the radical SiNC functionalization mechanism under most of the conditions applied.

Does the monomer concentration matter?

A high reactivity of silyl radicals with vinylic compounds is known for molecular silanes and polymers.[40,41] We suggest that once the surface silyl radical has formed addition of the surface silyl radical to an alkene proceeds rapidly. If the substrate addition to the surface silyl radicals would determine the reaction rate, an increase of the SiNC functionalization rates should

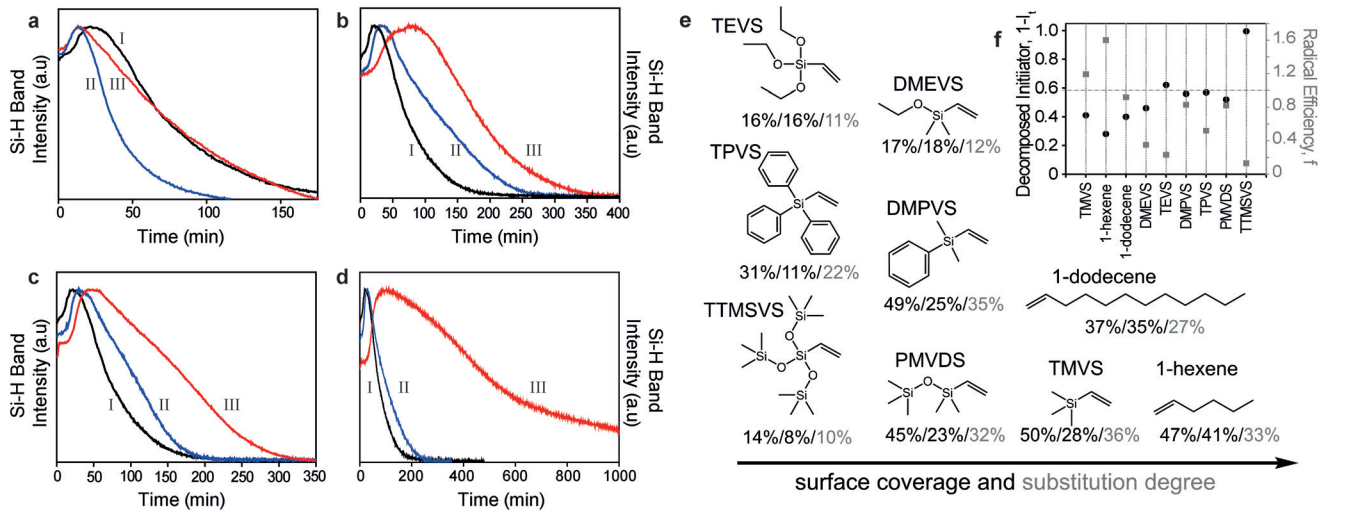

Fig. 4 Evolution of the SiH band intensity (2100 cm^{-1}) of SiNC functionalization at 70 °C with 6.8 μmol mL^{-1} AIBN in toluene (total volume: 3.6 mL). All figures show TMVS grafting (I) in comparison with functionalization using (a) 1-olefins: hexene (II) and dodecene (III); (b) phenylvinylsilanes: DMPVS (II), TPVS (III); (c) ethoxyvinylsilanes: DMEVS (II), TEVS (III); (d) siloxyvinylsilanes: PMVDS (II) and TTMSVS (III). (e) Surface coverage obtained from elemental analysis/TGA/molar Si–H substitution degree (grey). (f) Calculated relative amounts of decomposed initiators and radical efficiencies (ESI Table S11†) for applied substrates.

be observed in the *in situ* IR traces at higher monomer concentrations. This is not the case: the overall reaction rate does slow down with increasing monomer concentration (ESI Table S2,† entry 4). The major disparities, however, are observed in the regime where the agglomerates are large (Fig. 5a), which probably arise from poorer dispersibility in the neat substrates. Once the agglomerates are broken up, the decrease of the Si–H IR-signal (*e.g.*, Fig. 5a, trace IV) with increasing reaction time shows a similar slope to the traces I–III. Thus, the monomer addition to the $Si^{\bullet}$ surface radicals cannot be the rate determining step, and the progress should be strictly driven by the radical concentrations and alkene structure.

To further investigate the dependence of the reaction on the presence of radicals, the SiNC functionalization with TMVS was interrupted by abrupt cooling of the reaction mixture from 70 °C to room temperature (r.t., Fig. 5b). At r.t., the Si–H signal intensity and, accordingly, the concentration of surface Si–H bonds remains constant. The reaction proceeds when reheated to 70 °C due to the fast generation of new radicals. The same reactivity has also been found when benzene was used as solvent, which is known as a weak radical transfer agent (ESI Fig. S1d†), indicating that the H-abstraction from the present substrate molecules is favored over the abstraction from solvent molecules. Both cases show that the reaction kinetics strictly depend on the presence of radicals in solution.

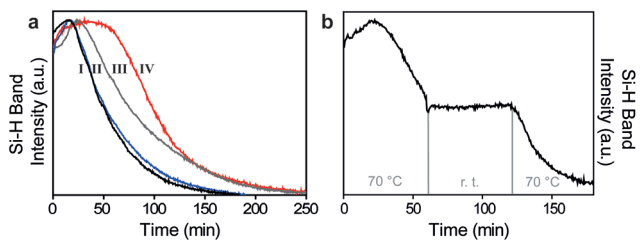

Fig. 5 (a) Time resolved *in situ* IR measurement of the Si–H band using 6.8 μmol mL^{-1} AIBN in toluene at TMVS concentrations of 1.26 mmol mL^{-1} (I), 0.63 mmol mL^{-1} (II), 2.52 mmol mL^{-1} (III) or neat (IV) TMVS. (b) Time resolved evolution of the Si–H bond of SiNCs using AIBN and TMVS in toluene. At 60 min, the temperature was decreased to room temperature using a water bath and reheated to 70 °C for 120 min.

Conclusions

In situ IR spectroscopy was used to follow the radical grafting process of hydride terminated SiNCs with unsaturated substrates. SiNC dispersions become clear during the functionalization with such olefins due to a break up of agglomerates, which has mostly been accepted as the end of the functionalization reaction. Here, we demonstrated that after clearing of the reaction solution, the surface functionalization of the individual SiNCs is far from being complete. The time difference between clearing of the dispersion and the finalization of the reaction arises with the bulkiness of the substrates. Furthermore, we observed that the hydrosilylation on SiNC surfaces is strongly dependent on the radical initiator concentration, the reaction temperature and the sterics of the alkenes applied; it is not related to the monomer concentration. Generally, radical efficiencies of the SiNC functionalization can exceed unity.

Acknowledgements

IRTG 2022 "ATUMS" (DFG) and NSERC are thanked gratefully for research funding. J. K. thanks TUM Graduate School for financial support. T. H. thanks the Studienstiftung des

deutschen Volkes and IGGSE for financial support. Dr Carsten Troll is thanked for support with the technical equipment. We thank our groups for helpful discussions.

Notes and references

1 Z. Ding, B. M. Quinn, S. K. Haram, L. E. Pell, B. A. Korgel and A. J. Bard, Electrochemistry and Electrogenerated Chemiluminescence from Silicon Nanocrystal Quantum Dots, *Science*, 2002, **296**, 1293–1297, DOI: 10.1126/science.1069336.

2 J. Liu, F. Erogbogbo, K.-T. Yong, L. Ye, J. Liu, R. Hu, H. Chen, Y. Hu, Y. Yang, J. Yang, I. Roy, N. A. Karker, M. T. Swihart and P. N. Prasad, Assessing clinical prospects of silicon quantum dots: studies in mice and monkeys, *ACS Nano*, 2013, **7**, 7303–7310, DOI: 10.1021/nn4029234.

3 S. Regli, J. A. Kelly, A. M. Shukaliak and J. G. C. Veinot, Photothermal Response of Photoluminescent Silicon Nanocrystals, *J. Phys. Chem. Lett.*, 2012, **3**, 1793–1797, DOI: 10.1021/jz3004766.

4 M. Dasog, K. Bader and J. G. C. Veinot, Influence of Halides on the Optical Properties of Silicon Quantum Dots, *Chem. Mater.*, 2015, **27**, 1153–1156, DOI: 10.1021/acs.chemmater.5b00115.

5 A. Angı, R. Sinelnikov, A. Meldrum, J. G. C. Veinot, I. Balberg, D. Azulay, O. Millo and B. Rieger, Photoluminescence through in-gap states in phenylacetylene functionalized silicon nanocrystals, *Nanoscale*, 2016, **8**, 7849–7853.

6 M. Dasog, J. Kehrle, B. Rieger and J. G. C. Veinot, Silicon Nanocrystals and Silicon-Polymer Hybrids: Synthesis, Surface Engineering, and Applications, *Angew. Chem., Int. Ed.*, 2016, **55**, 2322–2339, DOI: 10.1002/anie.201506065.

7 R. Ban, F. Zheng and J. Zhang, A highly sensitive fluorescence assay for 2,4,6-trinitrotoluene using amine-capped silicon quantum dots as a probe, *Anal. Methods*, 2015, **7**, 1732–1737, DOI: 10.1039/C4AY02729A.

8 C. M. Gonzalez, M. Iqbal, M. Dasog, D. G. Piercey, R. Lockwood, T. M. Klapotke and J. G. C. Veinot, Detection of high-energy compounds using photoluminescent silicon nanocrystal paper based sensors, *Nanoscale*, 2014, **6**, 2608–2612, DOI: 10.1039/C3NR06271F.

9 X. Cheng, S. B. Lowe, S. Ciampi, A. Magenau, K. Gaus, P. J. Reece and J. J. Gooding, Versatile "click chemistry" approach to functionalizing silicon quantum dots: applications toward fluorescent cellular imaging, *Langmuir*, 2014, **30**, 5209–5216, DOI: 10.1021/la500945f.

10 Y. Zhai, M. Dasog, R. B. Snitynsky, T. K. Purkait, M. Aghajamali, A. H. Hahn, C. B. Sturdy, T. L. Lowary and J. G. C. Veinot, Water-soluble photoluminescent d-mannose and l -alanine functionalized silicon nanocrystals and their application to cancer cell imaging, *J. Mater. Chem. B*, 2014, **2**, 8427–8433, DOI: 10.1039/C4TB01161A.

11 F. Erogbogbo, K.-T. Yong, I. Roy, R. Hu, W.-C. Law, W. Zhao, H. Ding, F. Wu, R. Kumar, M. T. Swihart and P. N. Prasad, In Vivo Targeted Cancer Imaging, Sentinel Lymph Node Mapping and Multi-Channel Imaging with Biocompatible Silicon Nanocrystals, *ACS Nano*, 2010, **5**, 413–423, DOI: 10.1021/nn1018945.

12 B. Ghosh, Y. Masuda, Y. Wakayama, Y. Imanaka, J. Inoue, K. Hashi, K. Deguchi, H. Yamada, Y. Sakka and S. Ohki, Hybrid white light emitting diode based on silicon nanocrystals, *Adv. Funct. Mater.*, 2014, **24**, 7151–7160.

13 F. Maier-Flaig, J. Rinck, M. Stephan, T. Bocksrocker, M. Bruns, C. Kübel, A. K. Powell, G. A. Ozin and U. Lemmer, Multicolor silicon light-emitting diodes (SiLEDs), *Nano Lett.*, 2013, **13**, 475–480, DOI: 10.1021/nl3038689.

14 T. Lin, X. Liu, B. Zhou, Z. Zhan, A. N. Cartwright and M. T. Swihart, A Solution-Processed UV-Sensitive Photodiode Produced Using a New Silicon Nanocrystal Ink, *Adv. Funct. Mater.*, 2014, **24**, 6016–6022, DOI: 10.1002/adfm.201400600.

15 A. Shiohara, S. Hanada, S. Prabakar, K. Fujioka, T. H. Lim, K. Yamamoto, P. T. Northcote and R. D. Tilley, Chemical reactions on surface molecules attached to silicon quantum dots, *J. Am. Chem. Soc.*, 2010, **132**, 248–253, DOI: 10.1021/ja906501v.

16 M. G. Panthani, C. M. Hessel, D. Reid, G. Casillas, M. José-Yacamán and B. A. Korgel, Graphene-Supported High-Resolution TEM and STEM Imaging of Silicon Nanocrystals and their Capping Ligands, *J. Phys. Chem. C*, 2012, **116**, 22463–22468, DOI: 10.1021/jp308545q.

17 M. Guan, W. Wang, E. J. Henderson, O. Dag, C. Kübel, V. S. K. Chakravadhanula, J. Rinck, I. L. Moudrakovski, J. Thomson, J. McDowell, A. K. Powell, H. Zhang and G. A. Ozin, Assembling photoluminescent silicon nanocrystals into periodic mesoporous organosilica, *J. Am. Chem. Soc.*, 2012, **134**, 8439–8446, DOI: 10.1021/ja209532e.

18 C. M. Hessel, E. J. Henderson and J. G. C. Veinot, Hydrogen Silsesquioxane: A Molecular Precursor for Nanocrystalline Si–SiO 2 Composites and Freestanding Hydride-Surface-Terminated Silicon Nanoparticles, *Chem. Mater.*, 2006, **18**, 6139–6146, DOI: 10.1021/cm0602803.

19 Z. Yang, M. Iqbal, A. R. Dobbie and J. G. C. Veinot, Surface-Induced Alkene Oligomerization: Does Thermal Hydrosilylation Really Lead to Monolayer Protected Silicon Nanocrystals?, *J. Am. Chem. Soc.*, 2013, **135**, 17595–17601, DOI: 10.1021/ja409657y.

20 J. A. Kelly and J. G. C. Veinot, An Investigation into Near-UV Hydrosilylation of Freestanding Silicon Nanocrystals, *ACS Nano*, 2010, **4**, 4645–4656, DOI: 10.1021/nn101022b.

21 J. A. Kelly, A. M. Shukaliak, M. D. Fleischauer and J. G. C. Veinot, Size-Dependent Reactivity in Hydrosilylation of Silicon Nanocrystals, *J. Am. Chem. Soc.*, 2011, **133**, 9564–9571, DOI: 10.1021/ja2025189.

22 Z. Yang, C. M. Gonzalez, T. K. Purkait, M. Iqbal, A. Meldrum and J. G. C. Veinot, Radical Initiated Hydrosilylation on Silicon Nanocrystal Surfaces: An Evaluation of Functional Group Tolerance and Mechanistic Study, *Langmuir*, 2015, **31**, 10540–10548, DOI: 10.1021/acs.langmuir.5b02307.

23 I. M. D. Höhlein, J. Kehrle, T. Helbich, Z. Yang, J. G. C. Veinot and B. Rieger, Diazonium Salts as Grafting Agents and Efficient Radical-Hydrosilylation Initiators for Freestanding Photoluminescent Silicon Nanocrystals, *Chem. – Eur. J.*, 2014, **20**, 4212–4216, DOI: 10.1002/chem.201400114.

24 X. Cheng, S. B. Lowe, P. J. Reece and J. J. Gooding, Colloidal silicon quantum dots: from preparation to the modification of self-assembled monolayers (SAMs) for bio-applications, *Chem. Soc. Rev.*, 2014, **43**, 2680, DOI: 10.1039/c3cs60353a.

25 Y. Wang, H. Wang, J. Guo, J. Wu, L. J. Gao, Y. H. Sun, J. Zhao and G. F. Zou, Water-Soluble Silicon Quantum Dots with Quasi-Blue Emission, *Nanoscale Res. Lett.*, 2015, **10**, 1012, DOI: 10.1186/s11671-015-1012-2.

26 J. Kehrle, I. M. D. Höhlein, Z. Yang, A.-R. Jochem, T. Helbich, T. Kraus, J. G. C. Veinot and B. Rieger, Thermoresponsive and photoluminescent hybrid silicon nanoparticles by surface-initiated group transfer polymerization of diethyl vinylphosphonate, *Angew. Chem., Int. Ed.*, 2014, **53**, 12494–12497, DOI: 10.1002/anie.201405946.

27 M. P. Stewart and J. M. Buriak, Exciton-mediated hydrosilylation on photoluminescent nanocrystalline silicon., *J. Am. Chem. Soc.*, 2001, **123**, 7821–7830.

28 J. M. Buriak, Organometallic Chemistry on Silicon and Germanium Surfaces, *Chem. Rev.*, 2002, **102**, 1271–1308, DOI: 10.1021/cr000064s.

29 B. J. Eves, Q.-Y. Sun, G. P. Lopinski and H. Zuilhof, Photochemical Attachment of Organic Monolayers onto H-Terminated Si(111): Radical Chain Propagation Observed via STM Studies, *J. Am. Chem. Soc.*, 2004, **126**, 14318–14319, DOI: 10.1021/ja045777x.

30 M. R. Linford and C. E. D. Chidsey, Alkyl monolayers covalently bonded to silicon surfaces, *J. Am. Chem. Soc.*, 1993, **115**, 12631–12632.

31 M. R. Linford, P. Fenter, P. M. Eisenberger and C. E. D. Chidsey, Alkyl monolayers on silicon prepared from 1-alkenes and hydrogen-terminated silicon, *J. Am. Chem. Soc.*, 1995, **117**, 3145–3155.

32 J. Holm and J. T. Roberts, Thermally Induced Hydrosilylation at Deuterium-Terminated Silicon Nanoparticles: An Investigation of the Radical Chain Propagation Mechanism, *Langmuir*, 2009, **25**, 7050–7056, DOI: 10.1021/la8042236.

33 L. F. Cason and H. G. Brooks, An Interesting Side-Reaction in the Preparation of Triphenylvinylsilane 1a, *J. Am. Chem. Soc.*, 1952, **74**, 4582–4583, DOI: 10.1021/ja01138a039.

34 R. Nagel and H. W. Post, Studies in Silico-Organic Compounds. XXI. Alkyl and Phenyl Derivatives of vinyltrichlorosilane, *J. Org. Chem.*, 1952, **17**, 1379–1381, DOI: 10.1021/jo50010a016.

35 D. Seyferth and D. L. Alleston, The Cleavage of Hexamethyldisiloxane and Hexamethyldigermoxane by Methyllithium: A Convenient Preparation of Lithium Trimethylsilanolate and Lithium Trimethylgermanolate, *Inorg. Chem.*, 1963, **2**, 418–420, DOI: 10.1021/ic50006a048.

36 T. Iimura, S. Onodera, T. Okawa and M. Yoshitake, WO2003064436 A1, 2003.

37 I. M. D. Höhlein, J. Kehrle, T. K. Purkait, J. G. C. Veinot and B. Rieger, Photoluminescent silicon nanocrystals with chlorosilane surfaces - synthesis and reactivity, *Nanoscale*, 2015, **7**, 914–918, DOI: 10.1039/C4NR05888G.

38 T. M. Stefanac, M. A. Brook and R. Stan, Radical Reactivity of Hydrovinylsilanes: Homooligomers, *Macromolecules*, 1996, **29**, 4549–4555, DOI: 10.1021/ma951495t.

39 J. Brandrup, E. H. Immergut and E. A. Grulke, *Polymer handbook*, Wiley, New York, Chichester, 4th edn, 2004.

40 S. Koltzenburg, M. Maskos and O. Nuyken, *Polymere: Synthese*, Eigenschaften und Anwendungen, Springer Spektrum, Berlin, 1st edn, 2014.

41 G. Odian, *Principles of Polymerization*, John Wiley and Sons, New Jersey, 4th edn, 2004.

42 C. Chatgilialoglu, Structural and Chemical Properties of Silyl Radicals, *Chem. Rev.*, 1995, **95**, 1229–1251, DOI: 10.1021/cr00037a005.